Electronic Supplementary Material (ESI) for Analytical Methods.

Electronic Supplementary Information

Multiple heteroatom-doped photoluminescent carbon dots for ratiometric detection of Hg^{2+} ions in cell imaging and environmental applications

Sonaimuthu Mohandoss,[a] Hari Datta Khanal,[a] Subramanian Palanisamy,[b] SangGuan You,[b] Jae-Jin Shim,[a] and Yong Rok Lee[a,*]

[a]School of Chemical Engineering, Yeungnam University, Gyeongsan, Gyeongbuk-do 38541, Republic of Korea.

[b]Department of Marine Food Science and Technology, Gangneung-Wonju National University, 120 Gangneungdaehangno, Gangneung, Gangwon 25457, Republic of Korea.

*Corresponding author: Yong Rok Lee (E-mail: yrlee@yu.ac.kr)

Table of contents

1. Characterization

The molecules were registered with a UV 3220 spectrometer (Optizen) or a spectrometer (HITACHI) F-2700 with a Xe Arc Lamp in ultraviolet-visible (UV–Vis) and fluorescence spectra respectively. The pH values of solutions were measured using 720P pH meter (Istek instruments). The FT-IR spectra were recorded using an FT-IR spectrometer (Perkin Elmer) in the range of 4000–400 cm^{-1}. The diffraction study was conducted using a 5° min^{-1} scanning speed with a wavelength of 1,5405 Å was performed with a 10-80° range of X-ray diffractometer (XRD) (PANalytic X'Pert Philips, MRD model). Raman spectroscopy was performed to investigate the SERS behaviors of substrates using a Raman (Horiba HR Evolution 800) spectrometer with 532 nm laser wavelength, 48 mW laser power, 1200 gr/mm diffraction grid, and 500 nm spatial resolution at the core research support center for natural products and medical materials, Yeungnam University. X-ray photoelectron spectroscopy (XPS, Thermo Fisher, USA.) measurements were obtained using Multilab-2000 spectrometer with Al Kα radiation monochromatized source. High-resolution and transmission electron microscopy (HRTEM and TEM) images were recorded (JEOL JEM-2100) with an accelerating voltage of 200 kV. The specimens used for TEM were prepared by evaporating one drop of the sample solution on lacy grids, followed by drying at room temperature.

2. Calculation of the photoluminescence quantum yield

Quinine sulfate with a QY of 54% at 425 nm was used as the reference to calculate the QY of NSB-CDs. Quinine sulfate and NSB-CDs were dissolved at a series of concentrations in 0.1 M H_2SO_4 (refractive index $\eta = 1.33$) and ultrapure water ($\eta = 1.33$) respectively for absorbance and photoluminescence measurements at the excitation wavelength of 425 nm. To minimize the self-absorption effect, the absorbance of each solution was below 0.1. After that, solutions

for absorption and emission measurements were carried out in a 1 x 1 cm quartz cuvette. Quantum yield (QY) was measured using a fluorescence spectrophotometer F-7000 (Hitachi). The QY of NSB-CDs was calculated by the following Eq.

$$QY = QY_R \cdot (k/k_R) \cdot (\eta/\eta_R)^2$$

where k is the slope of the linear fitted curve with integrated photoluminescence intensity versus absorbance; η is the solvent refractive index. The subscript R stands for reference (quinine sulfate).

3. Stability of the NSB-CDs

During the stability of NSB-CDs (20 μg mL^{-1}), we used different solvents and pH stability of the NSB-CDs solution investigated by adding HCl (0.1 M) or NaOH (0.1 M) aqueous solution to tune the pH values (1–14). As for NaCl salt ionic strength stability was introduced into the NSB-CDs solution at the concentration range from 0 to 1.0 M. The NSB-CDs solution was continuously irradiated at the wavelength of 425 nm for 120 min, during which the photoluminescence intensity was monitored every minute to evaluate the photostability. After 2 min of incubation, the photoluminescence spectrum of NSB-CDs was collected under excitation at 425 nm. Accordingly, the corresponding fluorescence intensities were measured at room temperature. All measurements were conducted in triplicate and then averaged.

4. Calculation of the association constant and stoichiometry

The association constant (K_a) of NSB-CDs/Hg^{2+} complex was determined by the Benesi–Hildebrand plot Eq.

$$\frac{1}{P - P_0} = \frac{1}{K_a \times [P_{max} - P_0] \times [Hg^{2+}]} + \frac{1}{P_{max} - P_0}$$

where P_0 and P are the PL intensity at 496 nm in the absence and presence of Hg^{2+} ions, and

P_{max} is the maxima PL intensity at 496 nm in the presence of Hg^{2+} in an aqueous solution. The association constant (K_a) was calculated graphically by plotting $1/(P - P_0)$ against $1/[Hg^{2+}]$. Data were linearly fitted by the following equation and the K_a value was obtained from the slope and intercept of the line. The binding stoichiometry of the NSB-CDs/Hg^{2+} complex was determined from a Jobs plot analysis. An aqueous solution containing NSB-CDs (20 μg mL^{-1}) and HEPES buffer solution (10 mM, pH 7.4) of $HgCl_2$ were prepared individually. After that, adjusting the NSB-CDs mole ratio from 0.1 to 0.9 in such a way that the total Hg^{2+} ion and NSB-CDs volume remained constant (2.0 mL). The total concentration of NSB-CDs and Hg^{2+} ions was kept constant. After vortex mixing the samples for 5 min, photoluminescence emission peaks were analyzed with a fluorescent spectrometer.

5. Solvatochromic studies of the NSB-CDs

The solvatochromic properties of NSB-CDs dissolved in acetone, acetonitrile, diethyl ether, 1,4-dioxane, N, N-dimethylformamide, dimethyl sulfoxide, ethanol, ethyl acetate, methanol, and water were examined to determine the effect of the solvent-dependent photoluminescence (PL) emission behavior, as shown in Fig. S1.[1] PL active compounds display redshifts in their emission spectra when the polarity of the surrounding medium changes, according to general tendencies. In the presence of water, however, the dual emissive NSB-CDs exhibited hypsochromic emission shifts (polar solvent). This suggests that the synthesized NSB-CDs do not interfere with the PL activity and exhibit high solubility in widely used solvents (Fig. S1a).[2] In water, the emission maxima was a pronounced peak because of the significant hydrogen-bonding interactions, dipole-dipole interactions, and particular solute-solvent interactions. In the DMF, DMSO, and THF solvents, a bathochromic shift was noted between the NSB-CDs, but the particular interactions were less pronounced, causing the dual emission maxima to

appear as a shoulder band. Under UV illumination, the redshift could be seen with the naked eye, as shown in Fig. S1b.[3]

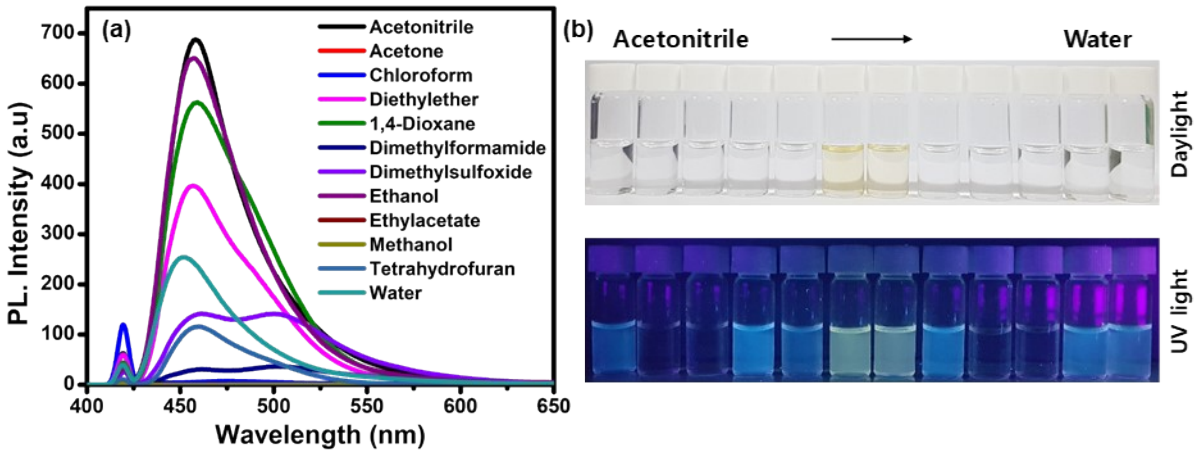

Figure S1. (a) Photoluminescence spectra of NSB-CDs using various solvents. (b) photographs of NSB-CDs in various solvents under daylight and 365 nm UV lamp.

6. Photoluminescence stability of the NSB-CDs

To verify the stability of NSB-CDs, we measured the effects of pH levels, NaCl salt ionic strength, irradiation time, and long-term storage on PL intensity as shown in Fig. S2. The PL signals of NSB-CDs under a large range of pH (1.0-14.0) were obtained in Fig. S2a. The PL intensity of NSB-CDs is nearly unchanged when pH is the change from 2.0 to 10.0 and quenching PL intensity when pH rises from 10.0 to 14.0.[4] The protonation and deprotonation (-NH_2, -OH, -COOH, and –SO_3H) mechanisms of the functional groups on the surface of the NSB-CDs may be attributed to the PL intensity of the NSB-CDs solutions, which shows the maximum at pH 7.0 and remains at over 95% in NSB-CDs solutions of pH 1.0 and pH 12.0 to 14.0. Because the human physiological pH is at 7.4, the intensity of the NSB-CDs is maintained at 90% of maximum when the pH is 7.0, assuring that the NSB-CDs can be used in biomedical applications. Afterward, the effect of ionic strength was examined by recording the PL spectra under various NaCl concentrations (Fig. S2b).[5] The ultrahigh concentration of NaCl rises to

1.0 M, the PL intensity is almost unchanged. The corresponding color changes of NSB-CDs in daylight under a UV lamp at 365 nm irradiation with the addition of pH and NaCl as shown in inset Fig. S2a,b. The PL intensity of NSB-CDs decreased slightly with increasing after continuous irradiation for 60 min (Fig. S2c). It was seen that the PL intensity only decreased by about 4% in 6 months under long-time storage at room temperature (Fig. S2d). Given this, we speculate that NSB-CDs have a good prospect of biological application applications in sensing, analysis, and cells imaging.

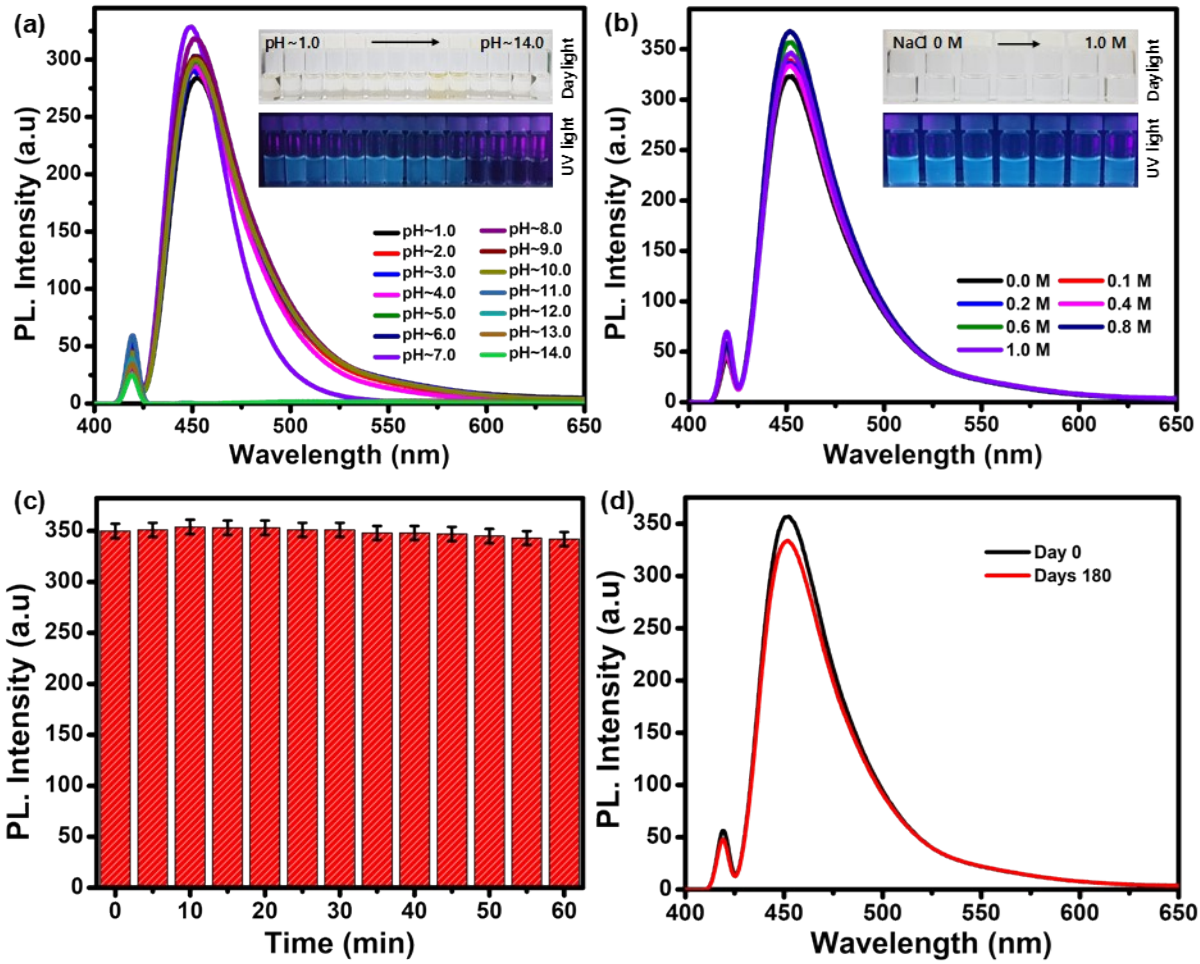

Figure S2. Photoluminescence spectra of NSB-CDs using different pH (1.0 – 14.0) (a) and NaCl salt ionic strength. Insert photographs, the corresponding color changes of NSB-CDs in daylight under a UV lamp at 365 nm irradiation with the addition of pH~1.0 – 14.0 and NaCl (0 – 1.0 M), (c) continuous irradiation time, and (d) long time room temperature storage on PL stability of the NSB-CDs.

7. Optimization of NSB-CDs towards Hg^{2+} ions

The quantum yields of NSB-CDs after adding the Hg^{2+} ions supported the PL enhancement. After adding Hg^{2+} ions, the quantum yield of NSB-CDs (17.6%) increased to 32.4% (Hg^{2+}).[6] The pH influence and response time of NSB-CDs toward Hg^{2+} ions were analyzed further (Figs. S3 and S4). Upon treatment with Hg^{2+} ions (30 μM), remarkable PL enhancement was observed at 496 nm that was kept almost unchanged over the wide pH range (4.0–11.0), as shown in Fig. S3.[7] As shown in Fig. S4, measurements of the kinetics of the PL intensity ratiometric variation of P_{496}/P_{452} showed that it was complete in four minutes, allowing it to be used as a ratiometric PL probe for the detection of Hg^{2+} ions.[8] These obvious changes are involved in forming a stable NSB-CDs/Hg^{2+} complex and influencing the PL response (Figs. S3 and S4). Therefore, the excellent selectivity of NSB-CDs toward Hg^{2+} ions over other ions is evident from the pronounced changes in the UV–vis and PL spectra. Consequently, pH ~ 7.4 makes the NSB-CDs suitable in biological systems. Fig. S4 shows the response time of NSB-CDs toward Hg^{2+} ions, from which the PL of NSB-CDs becomes stable in less than 5 min in the presence of Hg^{2+} ions.

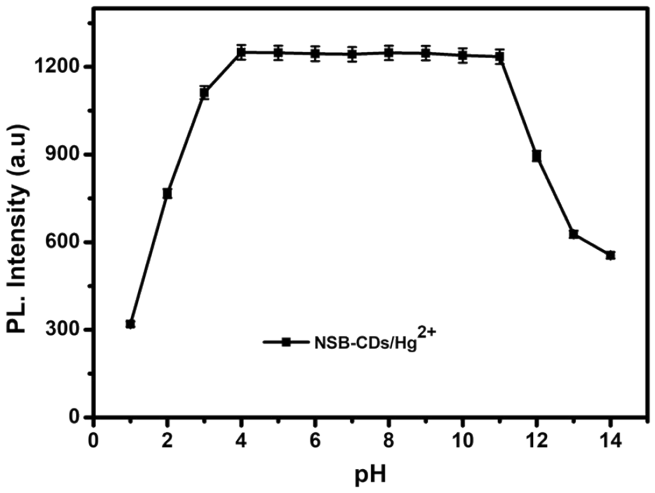

Figure S3. Photoluminescence intensity of chemosensor NSB-CDs (20 μg mL^{-1}) in presence of Hg^{2+} (30 μM) ~100 % aqueous solution at various pH values.

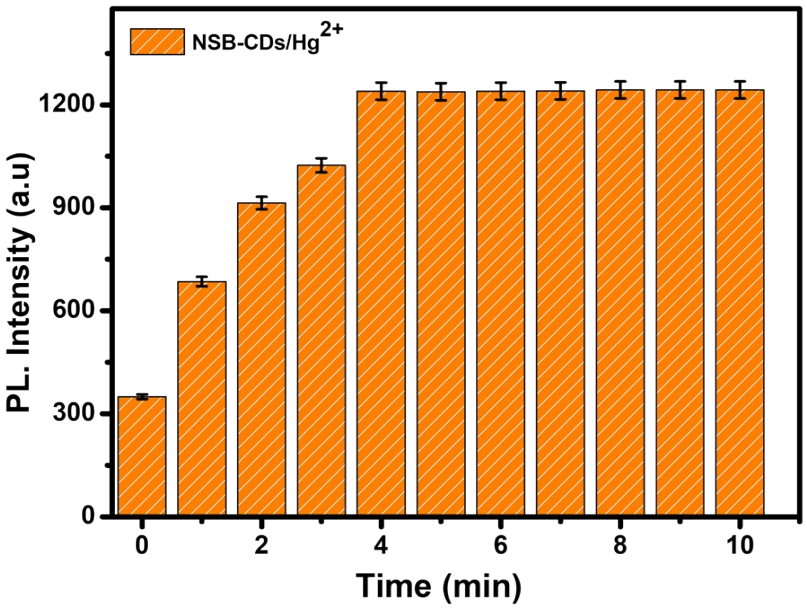

Figure S4. Time-dependent photoluminescence intensity of ratiometric chemosensor NSB-CDs (20 μg mL^{-1}) in presence of Hg^{2+} (30 μM) ~100 % aqueous solution (HEPES buffer, pH 7.4).

8. Stern-Volmer plot

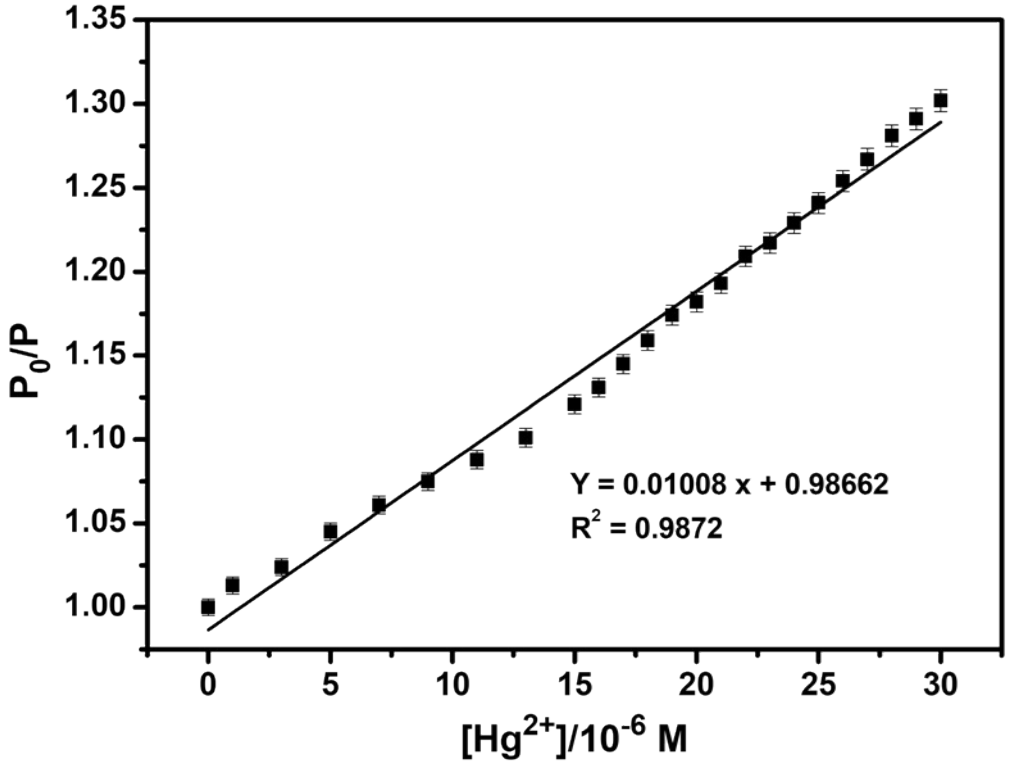

Figure S5. The Stern-Volmer plot response of the NSB-CDs intensity (P_0/P) to Hg^{2+} ions concentrations (0–30 μM).

9. Calculation of Limit of detection (LOD) and Limit of quantification (LOQ)

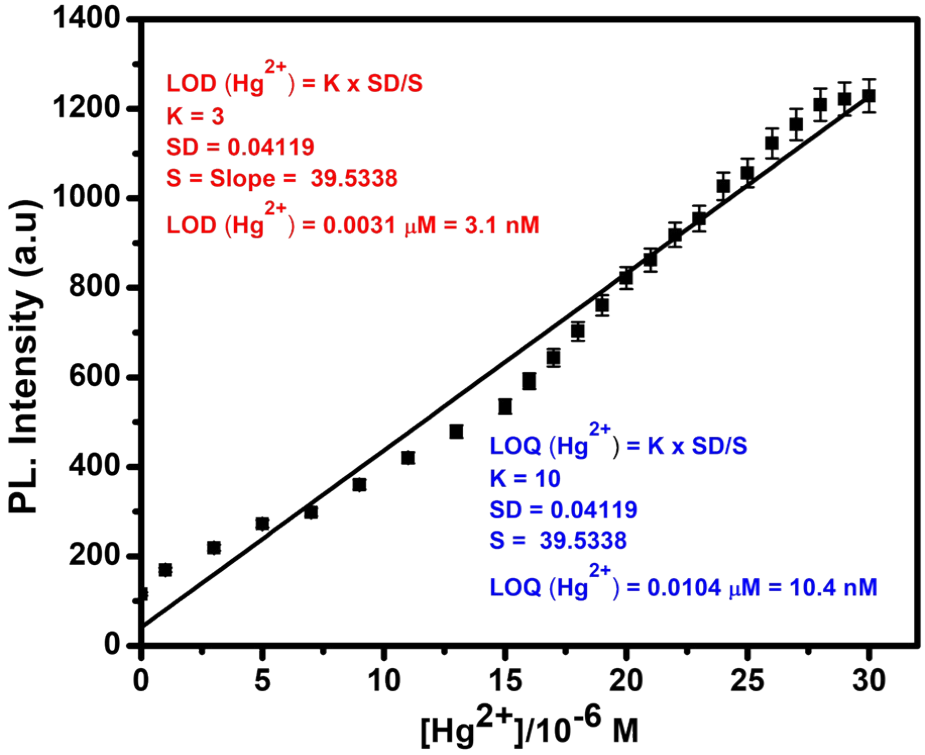

Figure S6. Calibration curve of NSB-CNs in the presence of Hg^{2+} ions using the monitored emission wavelength at 496 nm. The limit of detection (LOD) of Hg^{2+} ions was determined from the following equation: LOD and LOQ = K × SD/S, where K = 3 (LOD) and K = 10 (LOQ); SD is the standard deviation of the blank solution; S is the slope of the calibration curve.

10. Interference effect

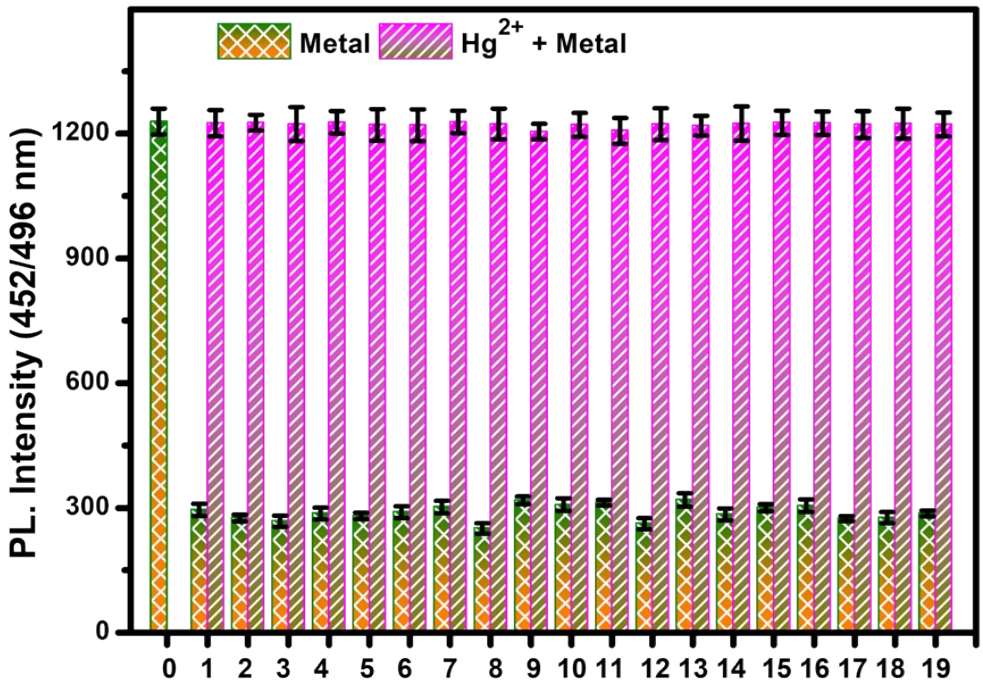

Figure S7. Interference effect of the histogram of NSB-CDs sensor upon the addition of various metal ions (Hg^{2+}, Ag^{+}, Ba^{2+}, Ca^{2+}, Cd^{2+}, Co^{2+}, Cu^{2+}, Al^{3+}, Cr^{3+}, Fe^{3+}, Ce^{3+}, Ir^{3+}, Mg^{2+}, Mn^{2+}, Na^{+}, Ni^{2+}, Pb^{2+}, Sn^{2+}, Sr^{2+}, and Zn^{2+}) and in the presence of Hg^{2+} ions with addition of other metal ions (1;Ag^{+}, 2;Ba^{2+}, 3;Ca^{2+}, 4;Cd^{2+}, 5;Co^{2+}, 6;Cu^{2+}, 7;Al^{3+}, 8;Cr^{3+}, 9;Fe^{3+}, 10;Ce^{3+}, 11;Ir^{3+}, 12;Mg^{2+}, 13;Mn^{2+}, 14;Na^{+}, 15;Ni^{2+}, 16;Pb^{2+}, 17;Sn^{2+}, 18;Sr^{2+}, and 19;Zn^{2+}) in HEPES buffer solution (10 mM, pH 7.4).

11. Cell viability

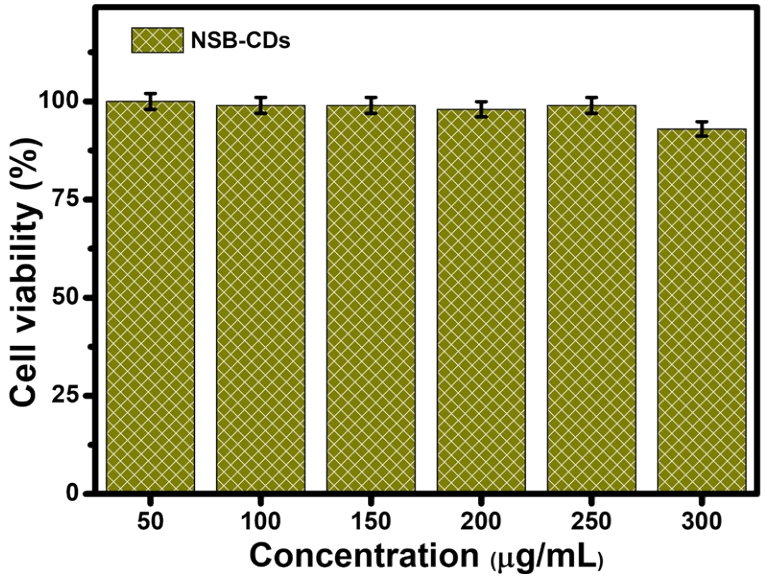

Figure S8. Cytotoxicity test of NSB-CDs on HCT-116 cells.

12. References

1 X. Shi, Y. Hu, H. M. Meng, J. Yang, L. Qu, X. B. Zhang and Z. Li, *Sens. Actuators B Chem.*, 2020, **306**, 127582.

2 A. Ekbote, S. M. Mobin and R. Misra, *J. Mater. Chem. C*, 2020, **8**, 3589–3602.

3 C. Fan, K. Ao, P. Lv, J. Dong, D. Wang, Y. Cai, Q. Wei and Y. Xu, *Nano*, 2018, **13**, 1–14.

4 S. W. Huang, Y. F. Lin, Y. X. Li, C. C. Hu and T. C. Chiu, *Molecules*, 2019, **24**, 1–12.

5 L. Li, L. Shi, J. Jia, O. Eltayeb, W. Lu, Y. Tang, C. Dong and S. Shuang, *Sens. Actuators B Chem.*, 2021, **332**, 129513.

6 P. A. Panchenko, A. V. Efremenko, A. V. Feofanov, M. A. Ustimova, Y. V. Fedorov and O. A. Fedorova, *Sensors (Switzerland)*, 2021, **21**, 1–15.

7 H. Guo, X. Wang, N. Wu, M. Xu, M. Wang, L. Zhang and W. Yang, *Anal. Chim. Acta*, 2021, **1141**, 13–20.

8 Y. Ge, A. Liu, R. Ji, S. Shen and X. Cao, *Sens. Actuators B Chem.*, 2017, **251**, 410–415.